Studies on the Effects of Truncating α-Helix E′ of p66 Human Immunodeficiency Virus Type 1 Reverse Transcriptase on Template−Primer Binding and Fidelity of DNA Synthesis†

Luis Menéndez-Arias*

Centro de Biología Molecular "Severo Ochoa", CSIC-Universidad Autónoma de Madrid, Cantoblanco, 28049 Madrid, Spain

Received July 29, 1998; Revised Manuscript Received September 24, 1998

ABSTRACT: The role of α-helix E′ of the RNase H domain of human immunodeficiency virus type 1 reverse transcriptase (HIV-1 RT) in template−primer binding and fidelity of DNA synthesis was investigated by using a series of mutant enzymes with deletions of 4, 8, 12, 16, and 20 amino acids at the C-terminal end of the 66 kDa subunit. The dissociation equilibrium constants (K_d) of wild-type HIV-1 RT and 38/16mer and 47/25mer DNA/DNA template−primer complexes were 2.2 ± 0.7 and 0.69 ± 0.35 nM, respectively. Deletions involving partial or total removal of α-helix E′ rendered enzymes with a 2−5-fold decrease in binding affinity. Misinsertion and mispair extension fidelity of DNA synthesis of the wild-type enzyme and truncated mutants were determined by using both DNA/DNA template−primers and a 47/25mer RNA/DNA complex. In all cases, incorporation assays were done in the same sequence context, which was taken from the viral *gag* gene. The removal of α-helix E′ had little effect on fidelity as determined with the three template−primers. Misinsertion fidelity assays showed that the specificity of mismatch formation was A:C ≈ A:G > A:A for the DNA template and A:C > A:G ≈ A:A for the RNA template, in 47/25mers. The specificity of extending mispaired 3′-termini was similar with both 47/25mers: A:C > A:A ≈ A:G. However, the efficiency of transversion mispair extension was higher with RNA templates. The results reported in this paper suggest that α-helix E′ may stabilize the RT/template−primer interaction, but does not have a strong influence in the correct positioning of the template−primer at the polymerase active site.

The human immunodeficiency virus type 1 (HIV-1)[1] reverse transcriptase (RT) is a virally encoded enzyme which converts the viral single-stranded RNA into double-stranded DNA which integrates into the host genome (*1*−*3*). It has two enzymatically distinct activities: a polymerase activity that synthesizes DNA using either RNA or DNA templates, and an endonuclease activity, termed RNase H, that degrades the RNA strand of RNA/DNA hybrids. HIV-1 RT lacks a 3′ exonucleolytic activity and is the most error-prone of known DNA polymerases (*4*−*6*). Its low fidelity contributes to the high genomic variability of HIV-1 and allows the virus to evade the host's immune system and to generate drug-resistant variants. The native enzyme exists as a heterodimer composed of two subunits of 66 and 51 kDa, termed p66 and p51, respectively (*7*, *8*). The p66 subunit, which is 560 residues in length, contains both the polymerase and the RNase H domains. The p51 subunit has the same amino acid sequence as p66, but lacks the 120 residues of the C-terminal region forming the RNase H domain. Besides, its DNA polymerase active site is buried and not accessible. Crystallographic studies have shown that the polymerase domains of both p66 and p51 contain four subdomains: fingers, palm, thumb, and connection (*7*). The three-dimensional structure of HIV-1 RT complexed with a 19/18mer double-stranded DNA showed that interactions involve the sugar−phosphate backbone of the nucleic acid and structural elements of fingers, palm, thumb, and RNase H domain of the 66 kDa subunit (*8*, *9*). The β12-β13 hairpin of p66 (residues 227−235) forms the "primer grip" and interacts with the 3′-terminal phosphates of the primer. Amino acid residues 76, 89, 151, 152, 154, and 157 have close contacts with the template strand and constitute the "template grip". In addition, the nucleic acid duplex is stabilized in the binding cleft by interactions involving α-helices H and I (residues 253−271 and 277−287 of p66, respectively), which form the so-called "helix clamp" (*10*). Further interaction sites were found in the RNase H domain, and involved residues of β-structure 1′, α-helices A′ and B′, and the loop containing His-539.

Alanine-scanning mutagenesis of residues Trp-229, Met-230, Gly-231, and Tyr-232 located at the β12-β13 hairpin which defines the primer grip led to significant alterations of DNA polymerase and RNase H activities. In the case of substitutions affecting Trp-229, Gly-231, or Tyr-232, the affinity of recombinant RT for template−primer is substan-

† This work was supported in part by Fondo de Investigación Sanitaria Grants 95/0034-01 and 98/0054-01 and an institutional grant of Fundación Ramón Areces, Madrid (Spain).

* To whom correspondence should be addressed. Tel: (34) 913978477. Fax: (34) 913974799. E-mail: lmenendez@cbm.uam.es.

[1] Abbreviations: HIV-1, human immunodeficiency virus type 1; RT, reverse transcriptase; RNase H, ribonuclease H; WT, wild-type; dNTP, deoxynucleoside triphosphate; SDS, sodium dodecyl sulfate; DTT, dithiothreitol; HEPES, 4-(2-hydroxyethyl)-1-piperazine-*N*′-2-ethanesulfonic acid; PEG, poly(ethylene glycol) 6000.

10.1021/bi981830g CCC: $15.00
Published on Web 11/04/1998

Table 1: Synthetic Oligonucleotides Used in the Mutagenesis of DNA Encoding the 66 kDa Subunit of HIV-1 RT

mutation[a]	oligodeoxynucleotide[b]
G541*	ATTTCCTCCAATTC**A**TTTGTGTGCTGG
N545*	ATCTACTTGTT**AT**T**A**TCCTCCAATTCCTTT
D549*	ACTGACAA**A**TTT**T**T**A**TACTTGTTCATTTCC
S553*	CCTGATTCCAGC**T**C**A**GACTAATTTATCTAC
R557*	TTCTAGTATTT**AT**C**A**GATTCCAGCACTGAC

[a] Mutations are identified by amino acid and position number in HIV-1 RT, followed by an asterisk to indicate the introduction of a termination codon at the indicated position. Amino acids are designated by the single-letter code. [b] Bold nucleotides correspond to mutations introduced in the RT coding region.

tially reduced, compromising viral infectivity (*11*−*13*). Several primer grip mutant RTs such as P226A, F227A, G231A, Y232A, E233A, and H235A displayed an altered RNase H phenotype, which could result from relocation of the template−primer in the nucleic acid binding cleft (*12*, *14*). The core of α-helix H (Gln-258, Gly-262, and Trp-266) interacts with the minor groove of the template−primer binding. Substitution of Gly-262 by Ala or Trp-266 by Ala or Thr rendered enzymes which showed altered template−primer binding properties, which affected catalytic cycling (*15*, *16*) and impaired their strand transfer and RNase H activities (*17*). Interestingly, mutants containing Ala at position 262 or 266 also showed a diminished frameshift fidelity as compared with the wild-type (WT) enzyme (*15*, *18*).

Modeling studies of HIV-1 RT with a DNA duplex region longer than 25 base pairs, and bearing a template−strand extension of at least 8 nucleotides (*19*), suggested that extended interactions with the template overhang were conferred by the β3-β4 hairpin of the fingers subdomain of p66. In addition, α-helix H-α-helix I hairpin of p51, together with α-helix E′ of p66 (residues 544−555) RNase H domain, was proposed to provide further stabilization for duplex DNA. A similar prediction was also reported for a 27 nucleotide double-stranded RNA fragment complexed with HIV-1 RT (*10*). The α-helix E′ contains the conserved Asp-549 which has been implicated in divalent metal ion coordination (*20*). It has been shown that deletions affecting α-helix E′ uncouple the endonuclease and directional processing activities of RT (*21*), and abolish virus infectivity (*22*). This paper deals with the effects of truncating α-helix E′ on template−primer binding and misinsertion and mispair extension fidelity of DNA synthesis. The data reported in this article suggest that the potential loss of contacts with α-helix E′ may not alter significantly the orientation and location of the template−primer within the binding cleft.

EXPERIMENTAL PROCEDURES

Mutagenesis. Site-directed mutagenesis was carried out with the Altered Sites in vitro mutagenesis system kit (Promega) as previously described (*23*). RT mutations and oligodeoxynucleotides used in the mutagenesis reaction are shown in Table 1. The introduced mutations were confirmed by DNA sequencing. Plasmids containing the mutated RTs were digested with *Nco*I and *Eco*RI, to isolate an insert of 1.7 kilobase pairs, which was then cloned in the expression vector pRT6 (*24*).

```
D2 / PG5 (38/16mer)

5′GGGATTAAATAAAATAGTAAGAATGTATAGCCCTACCA 3′
3′                          TACATATCGGGATGGT 5′
                           *

D2-47 / PG5-25 (47/25mer)

5′GGGATTAAATAAAATAGTAAGAATGTATAGCCCTACCAGCATTCTGG 3′
3′                          TACATATCGGGATGGTCGTAAGACC 5′
                           *

D2-47(RNA) / PG5-25 (47/25mer)

5′GGGAUUAAAUAAAAUAGUAAGAAUGUAUAGCCCUACCAGCAUUCUGG 3′
3′                          TACATATCGGGATGGTCGTAAGACC 5′
                           *
```

FIGURE 1: Nucleotide sequences of the DNA/DNA and RNA/DNA complexes used in the assays. Incorporation sites are indicated with an asterisk. Templates D2 and D2-47 mimick the HIV-1_{BH10} *gag* sequence and include nucleotides 915 (5′ end)-952 (3′ end) and 915 (5′ end)-961 (3′ end), respectively, according to the sequence numbering of GenBank accession number M15654.

Expression and Purification of HIV-1 RT Variants. Purification of mutant and WT RTs was carried out after independent expression of their subunits (p66 and p51) (*23*). The 51 kDa subunit was obtained with an extension of 14 amino acid residues at its N-terminal end, which includes six consecutive histidines to facilitate its purification by metal chelate affinity chromatography. Crystallographic studies have shown that the N-terminal of p51 is located away from the polymerase active site and does not participate in nucleic acid binding (*8*, *9*). In addition, we have previously reported that commercial heterodimeric RT lacking the polyhistidine tract displayed kinetic properties similar to those of the wild-type RT with the polyhistidine extension in p51 (*23*). All RTs were purified as p66/p51 heterodimers. The primary structure of p51 was identical in all of the mutants herein described. The purity of the enzymes was assessed by SDS−polyacrylamide gel electrophoresis. All enzymes were at least 95% pure. RT concentrations were estimated using the BioRad protein assay.

DNA Polymerase Activity Assays. Assays were carried out in 50 mM Tris-HCl (pH 8.0), 20 mM NaCl, 10 mM $MgCl_2$, 8 mM DTT, 5 μM dNTP (3−5 μCi/mL [^{3}H]dTTP or [8-^{3}H]dGTP), and 0.5 μM template−primer (concentration expressed as 3′-hydroxyl primer termini). Template−primer solutions of poly(rA)·oligo(dT)$_{12-18}$, poly(rC)·oligo(dG)$_{12-18}$, and poly(dC)·oligo(dG)$_{12-18}$ were prepared as previously described (*24*). Reactions (30 μL) were initiated by the addition of 0.2−2 pmol of enzyme, incubated at 37 °C for 10−30 min, and terminated by adding 20 μL of 0.5 M EDTA. The amount of polymerized deoxynucleotide was determined by acid-insoluble precipitation (*23*).

Determination of Dissociation Equilibrium Constants (K_d) by Nucleotide *Incorporation*. The template−primers used in these experiments are shown in Figure 1. Primer 5′ termini were labeled with [γ-^{32}P]ATP (10 mCi/mL, Amersham) and T4 polynucleotide kinase (Boehringer). The templates and the corresponding ^{32}P-labeled primers were annealed in 150 mM NaCl and 150 mM magnesium aspartate for 3 min at 90 °C, and then cooled slowly to room temperature. The template−primer concentration ratio was adjusted to 1:1 (2−3 μM concentration). Prior to the elongation reaction, template−primers were diluted 10-fold in 500 mM HEPES, pH 7.0, 150 mM NaCl, and 150 mM magnesium aspartate (final concentration). DNA/DNA and

RNA/DNA substrates (1−60 nM) were preincubated with WT RT or mutant derivatives in 25−50 μL of 100 mM HEPES, pH 7.0, 30 mM NaCl, 30 mM magnesium aspartate, 130 mM KCH_3COO, 1 mM DTT, and 5% PEG, at 37 °C for 10 min. RT concentrations in these experiments ranged from 0.5 to 2.5 nM for DNA/DNA substrates and were around 3−4 times higher for RNA/DNA duplexes. Reactions were initiated by the addition of an equal volume of a solution containing 0.2 mM dTTP, 130 mM KCH_3COO, 1 mM DTT, and 5% PEG. Aliquots were removed at different times and quenched with 0.6 volumes of stop solution (10 mM EDTA in 90% formamide containing 3 mg/mL xylene cyanol FF and 3 mg/mL bromophenol blue). Products were separated by 20% polyacrylamide−urea gel electrophoresis and quantified, as previously described (*25*). Incubations with different concentrations of template−primer were done in duplicate, and the amount of products synthesized in a single cycle of polymerization (burst amplitudes) was averaged for at least two sets of reactions and plotted with respect to the amount of template−primer initially reacted. The graph was fitted to the following equation:

$$[\mathrm{E{\cdot}TP}] = 0.5(K_d + E_T + \mathrm{TP}) - 0.5\sqrt{(K_d + E_T + \mathrm{TP})^2 - 4E_T\mathrm{TP}}$$

where [E·TP], K_d, E_T, and TP represent the productive RT/template−primer complex concentration, the equilibrium dissociation constant for RT−DNA binding, the active enzyme concentration, and the template−primer concentration, respectively (*26*, *27*). The percentage of active enzyme was determined as the ratio of E_T over total enzyme concentration, E_0, as determined spectrophotometrically.

Extension of Primers in the Presence of Three dNTPs. The DNA duplexes D2/PG5 and D2-47/PG5-25 (Figure 1) were used to determine the extent of misincorporation in the presence of only three dNTPs. Primers were ^{32}P-labeled at the 5′ end with T4 polynucleotide kinase, and template−primers were annealed and further diluted in HEPES-containing buffer as described above. The labeled template−primers at 20 nM (D2-47/PG5-25) or 30 nM (D2/PG5) were incubated with 50−100 nM RT at 37 °C for 30−45 min, in a total volume of 10 μL containing 50 mM HEPES, pH 7.0, 15 mM NaCl, 15 mM magnesium aspartate, 130 mM KCH3COO, 1 mM DTT, 5% PEG, and only three dNTPs at a concentration of 50 μM each (-G = dATP, dCTP, dTTP; -A = dCTP, dGTP, dTTP; -T = dATP, dCTP, dGTP; and -C = dATP, dGTP, dTTP). Each of the dNTPs used was of the highest purity grade, and they were supplied as 0.1 M solutions (Pharmacia). At the end of the incubation period the reactions were stopped by adding 8 μL of the EDTA−formamide stop solution described above. The reaction products were analyzed in denaturing 18% or 20% polyacrylamide−urea gels.

Misinsertion and Mispair Extension Fidelity Assays. Fidelity assays were performed essentially as previously described (*25*, *28*). Reaction conditions were the same as those used for the determination of dissociation equilibrium constants by nucleotide incorporation, except for the primers, the concentrations of dNTPs and RT, and the incubation times. The template−primers used in misinsertion fidelity assays are shown in Figure 1. For mispair extension fidelity assays we used six additional primers, which were ^{32}P-labeled at their 5′ end, and individually annealed to the corresponding templates. The nucleotide sequences of these primers were the following: PG5C (5′-TGGTAGGGCTATACAC-3′), PG5G (5′-TGGTAGGGCTATACAG-3′), PG5A (5′-TGGTAGGGCTATACAA-3′), PG5-25C (5′-CCAGAATGCTGGTAGGGCTATACAC-3′), PG5-25G (5′-CCAGAATGCTGGTAGGGCTATACAG-3′), and PG5-25A (5′-CCAGAATGCTGGTAGGGCTATACAA-3′). PG5C, PG5G, and PG5A were annealed to D2, and primers PG5-25C, PG5-25G, and PG5-25A were annealed either to D2-47 or to D2-47(RNA). These template−primers contain a mismatch at the 3′ end of the primer. Template−primer concentrations in the reaction mixtures were kept at 20 nM for D2-47-containing duplexes and 30 nM for duplexes having D2 or D2-47(RNA) as templates. The active enzyme concentration was around 5−15 nM in assays using DNA/DNA duplexes and 20−60 nM in assays with RNA/DNA template−primers. The rate of product formation was measured for 11−14 different concentrations of each correct or incorrect dNTP. Wherever possible, the incubation times were kept below the duration of one catalytic cycle (dissociation of the enzyme from position +1 followed by reassociation at position 0) (*29*). Therefore, in most assays, the incubation times for 47mer/25mer and 38mer/16mer duplexes were 20 and 30 s, respectively. However, extensions of approximately 10%−35% of the labeled primers at the highest triphosphate concentration were also obtained by using longer incubation periods (as, for example, in the case of A:G and A:A mismatches). Products were heat-denatured, resolved in 18% or 20% polyacrylamide−urea gels, and quantitated with a BAS 1500 scanner. Elongation measurements were fitted to the Michaelis−Menten equation, and the k_{cat} and K_m values were determined as previously described (*23*).

RNase H Activity Assays. The RNA template D2-47-(RNA) (30 pmol) was phosphorylated at its 5′ end with T4 polynucleotide kinase, annealed to 90 pmol of PG5-25 in 30 μL of 150 mM NaCl and 150 mM magnesium aspartate, and diluted 10-fold in 500 mM HEPES, pH 7.0, 150 mM NaCl, and 150 mM magnesium aspartate (final concentration). Reactions (50 μL) were carried out in 100 mM HEPES, pH 7.0, 30 mM NaCl, 30 mM magnesium aspartate, 130 mM KCH_3COO, 1 mM DTT, and 5% PEG. Reactions were initiated by adding 10 μL of the diluted hybrid solution to 40 μL of an RT solution at around 5−10 nM concentration. Samples were incubated at 37 °C, and aliquots were removed at appropriate times and mixed with 0.6 volumes of stop solution. The products were heat-denatured and analyzed in 18% polyacrylamide−urea gels. RNase H activity assays using homopolymeric template−primers were performed in the presence of $MgCl_2$, using [^{3}H]Poly(rA)·Poly(dT) as substrate, as previously described (*25*).

RESULTS

Mutants of Reverse Transcriptase. Truncated forms of the 66 kDa subunit of HIV-1 RT were obtained by introducing appropriately spaced stop codons at the 3′ end of the coding region of p66. This strategy lead to the partial or total removal of α-helix E′, which comprises residues 544−555 (*8*, *30*). Mutant 66 kDa subunits contained 540, 544, 548, 552, or 556 amino acids, instead of the 560 residues found in the WT p66. The mutant and the WT RTs were

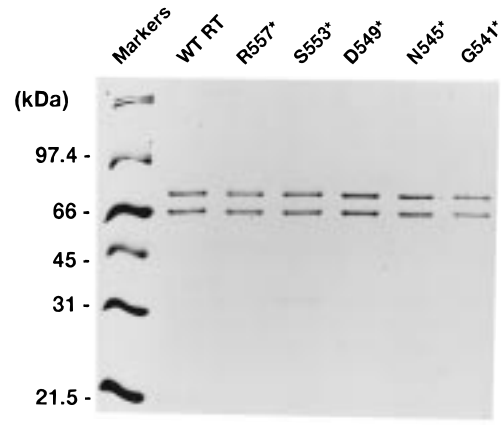

FIGURE 2: SDS−polyacrylamide gel electrophoresis of mutated HIV-1 RTs. Electrophoretic mobility of p66 and p51 is shown for the WT RT and the mutated enzymes. Molecular weight markers and their masses were the following: phosphorylase b (97.4 kDa), bovine serum albumin (66 kDa), ovalbumin (45 kDa), carbonic anhydrase (31 kDa), and soybean trypsin inhibitor (21.5 kDa).

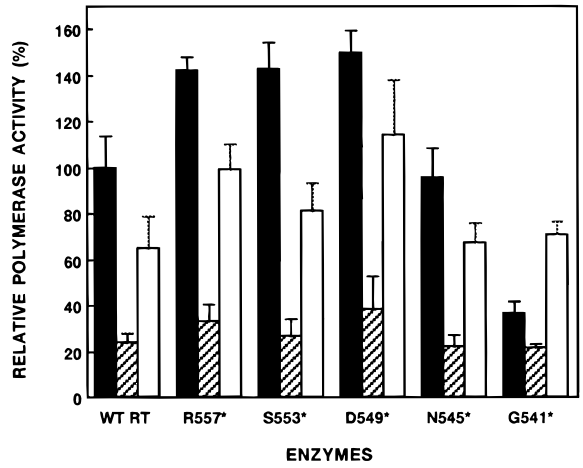

FIGURE 3: DNA polymerase activity of RTs with truncated 66 kDa subunits. Activities were determined with poly(rA)·oligo(dT)$_{12-18}$ (filled bars), poly(rC)·oligo(dG)$_{12-18}$ (dashed bars), and poly(dC)·oligo(dG)$_{12-18}$ (open bars) and normalized to the value obtained with the WT RT and poly(rA)·oligo(dT)$_{12-18}$. The specific activity of the WT enzyme was 1700 units/mg. One activity unit is the amount of enzyme that incorporates 1 nmol of [^{3}H]TMP into acid-insoluble products in 10 min at 37 °C under the conditions described in Materials and Methods.

prepared as p66/p51 heterodimers, after independent expression of their subunits. The 51 kDa subunit, which contains a polyhistidine tag in its amino-terminal region, was identical for all of the mutants characterized. Following purification, SDS−polyacrylamide gel electrophoretic analysis indicated that all mutant RT heterodimers were at least 95% pure (Figure 2). Densitometric analysis of the Coomassie blue stained bands revealed that the amount of p66 relative to p51 was always between 0.85 and 1.1, in agreement with the expected 1:1 subunit stoichiometry of the enzyme. All RT variants displayed significant DNA polymerase activity using homopolymeric template−primers (Figure 3).

Interaction with DNA/DNA Template−Primers. The first step of polymerization involves the physical association of the polymerase with its nucleic acid substrate. The equilibrium dissociation constant for WT HIV-1 RT and double-stranded DNA was determined from the amount of products synthesized in a single cycle of polymerization obtained with

Table 2: Dissociation Equilibrium Constants for WT and Mutant HIV-1 RTs and DNA/DNA Duplexes

enzymes	K_d (nM) (D2/PG5)	K_d (nM) (D2-47/PG5-25)
WT RT	2.2 ± 0.7	0.69 ± 0.35
R557*	2.4 ± 1.0	1.12 ± 0.58
S553*	5.0 ± 3.1	1.41 ± 0.51
D549*	5.7 ± 2.5	2.25 ± 0.82
N545*	8.8 ± 3.9	1.43 ± 0.58
G541*	12.7 ± 5.8	3.26 ± 2.20

different concentrations of DNA duplexes. Active site titrations were performed by preincubating a fixed concentration of RT with increasing concentrations of duplex DNA. The amount of enzyme bound to template−primer in the preincubation mixture was measured by adding dTTP and by following the linear time course of the subsequent reaction. The intercept with the *y* axis gave the amount of bound DNA at time 0. The K_d values obtained for the WT RT and DNA duplexes ranged from 0.65 to 2.1 nM, and were higher for the 38/16mer than for the 47/25mer. These values were consistent with those previously determined with a gel mobility shift assay (*23*). The comparison with the K_ds obtained for mutants having truncated forms of p66 is shown in Table 2. Interestingly, the removal of α-helix E′, as occurs in mutant G541*, leads to a small, but significant, reduction of the DNA binding affinity of the RT. In contrast, R557*, whose deletion does not affect α-helix E′, shows K_d values almost identical to those of the WT RT, using both template−primers.

Primer Extension Assays using Deoxynucleotide Templates and Biased dNTP Pools. An initial assessment of the fidelity of mutant HIV-1 RTs was obtained by using an assay that monitors primer extension in the presence of only three of four dNTPs complementary to template nucleotides. In these conditions, the elongation of the primer past a template nucleotide complementary to the deleted dNTP requires the insertion by the enzyme of an incorrect nucleotide and its further extension of the generated mismatch primer. The results are shown in Figure 4. In all reactions with WT and mutant RTs, a substantial accumulation of DNA products is observed at the site corresponding to the missing nucleotide. Extensions beyond these sites were hardly seen in the absence of dCTP. However, extensions beyond positions +1 and +4, respectively, were observed with both template−primers when dTTP or dATP were not included in the reaction mixture. This effect was most evident with the 47/25mer duplex, where large accumulations of extended primers of 32 nucleotides were observed with all enzymes in the absence of dATP. Although most of the enzymes tested showed similar extension patterns, differences were observed with mutants N545* and G541* and the template−primer D2-47/PG5-25. Image analysis of the obtained results revealed that 2−4 times less primer was elongated beyond the first stop site in both cases, and this effect was more pronounced with G541*. Taken together, the data of Figure 4 reveal that the replication accuracy of all mutants is roughly similar, although G541* and N545* could display a slightly higher fidelity in assays performed using longer template−primers.

Fidelity of DNA-Dependent DNA Synthesis. Steady-state kinetic parameters for incorporation of nucleotides at the 3′ end of the primer were obtained with template−primers D2/

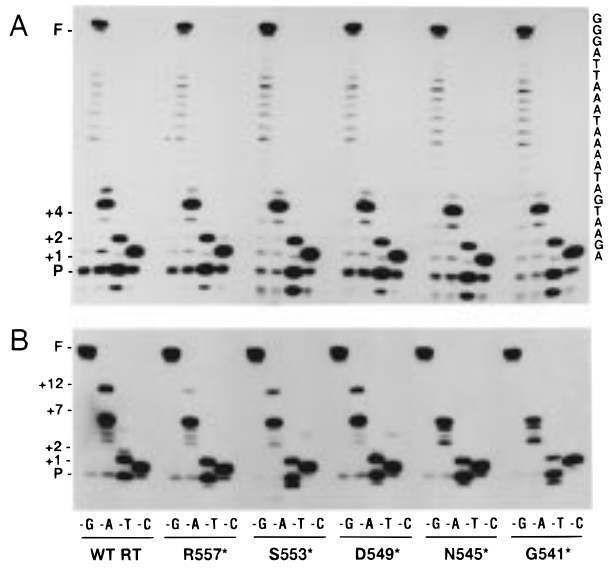

FIGURE 4: Primer extension by WT and mutant HIV-1 RTs in assays containing a deoxyoligonucleotide template and lacking a complementary dNTP. (A) shows the results of extension assays performed with the 38/16mer complex and (B) the results obtained with the 47/25mer complex. The lanes marked -G -A -T -C represent the missing fourth nucleotide from the dNTP mix in the respective set of experiments. The sequence of the single-stranded template extension is as shown to the right of (A). P indicates the position of the unextended primer, and F represents the fully extended product. The first stop sites of the reactions with only three nucleotides (+1, +2, +4) are one nucleotide shorter than the mismatched primers.

PG5 (38/16mer) and D2-47/PG5-25 (47/25mer) (Figure 1). The incorporation sites in both complexes are located in the same sequence context. Misinsertion and mispair extension fidelity assays were used to estimate the fidelity of RTs. Misinsertion fidelity assays involved kinetic measurements for the incorporation of a correct (T) or an incorrect (A, C, or G) nucleotide at the 3′ end of the primer. The results are shown in Table 3. Misinsertion efficiencies (f_{ins}) ranged from less than 2×10^{-6} to 6.0×10^{-5}. WT RT misinserted dCTP and dGTP with the highest efficiency, whereas there was hardly any extension in the presence of dATP. Similar results were obtained with both templates, using mutant G541*. Misincorporation efficiencies of G instead of T were determined for all enzymes and were found to be somewhat higher for the 38/16mer than for the 47/25mer. The f_{ins} values ranged from 2.8 to 6.0×10^{-5} for D2/PG5 and from 1.6 to 3.5×10^{-5} for D2-47/PG5-25. The kinetics of mispair extension were studied for correctly matched base pairs (A:T) and for mismatches A:C, A:G, and A:A. In all cases, we measured the incorporation of a correct T opposite of A at the 3′ end of the primer. The results are shown in Table 4. The A:C mispair was efficiently extended by all RTs in the context of both template−primers. Misextension efficiencies (f_{ext}) of A:C were estimated to be between 3.8×10^{-3} and 10.3×10^{-3} for all tested enzymes. The f_{ext} values for transversion mispairs (A:A or A:G) were below 2.2×10^{-5} in the case of D2-47/PG5-25, for the WT RT as well as for mutant G541*, which is devoid of α-helix E′. The low efficiency of mispair A:C extension is due to large increases of the K_m value, but in the case of transversion mispair extensions the effects on the k_{cat} become more significant.

Fidelity of RNA-Dependent DNA Synthesis. The fidelity properties of WT HIV-1 RT and G541* were compared using 47/25mer complexes containing an RNA or a DNA template. Fidelity of RNA-dependent DNA synthesis was estimated using the complex D2-47(RNA)/PG5-25 (Figure 1). The results obtained with the misinsertion (Table 5) and mispair extension fidelity assays (Table 6) were similar for WT HIV-1 RT and G541*. Both enzymes displayed a slightly different behavior when copying RNA or DNA templates. Thus, the incorporation of G instead of T at the 3′ end of the primer was around 10 times less efficient with the RNA template (see data in Tables 3 and 5), suggesting that purine/pyrimidine discrimination was more efficient in this context. On the other hand, the efficiency of A:C mispair extension was not influenced by the nature of the template, and transversion mispairs such as A:G and A:A were extended more efficiently using the RNA/DNA complex (Tables 4 and 6). The template−primer D2-47(RNA)/PG5-25 is a potential substrate of the endonuclease activity of HIV-1 RT. Before primer elongation, RNA/DNA complexes were incubated for 10 min with the enzyme, in the presence of Mg^{2+}. RNase H activity assays performed in the preincubation buffer conditions, using 5′-[^{32}P]-labeled D2-47(RNA), previously annealed to PG5-25, revealed that the RNA template was completely cleaved by the WT RT to a smaller species of around 36−38 nucleotides (data not shown). In contrast, the mutant G541* showed negligible endonuclease activity as determined using 5′-[^{32}P]-labeled D2-47(RNA)/PG5-25. Further support of this result was obtained from RNase H assays carried out with [^{3}H]Poly(rA)·Poly(dT). In these conditions, the RNase H specific activity of G541* was estimated to be less than 2% of the WT RT. Taken together, RNase H activity determinations and the data provided by the fidelity assays described above suggest that the endonucleolytic cleavage of the RNA template does not have a strong influence in the kinetics of misincorporation and mispair extension at the 3′ end of the primer.

DISCUSSION

Crystallographic data of the structure of HIV-1 RT complexed with double-stranded DNA revealed that the polymerase and the RNase H active sites are separated by approximately 17−18 nucleotides (*8*), an estimate which is in good agreement with reported biochemical data (*19*, *31*−*34*). However, modeling studies suggest that the RT replication complex can accommodate a double-stranded nucleic acid of at least 25 base pairs (*19*). Factors improving the stability of RT/template−primer interaction are the length of the 5′ overhang of the template strand (*27*), the number of base pairs involved in the double-stranded region formed by primer and template (*35*), and the presence of Mg^{2+} ions (*36*, *37*). The results obtained with the WT RT revealed that the enzyme binds 38/16mer and 47/25mer duplexes with high affinity, displaying K_d values similar to those reported for other heteropolymeric template−primers (*27*, *38*, *39*). The dissociation equilibrium constant for WT RT and the 47/25mer was around 2−3-fold higher than for the 38/16mer, suggesting that extension of 9 nucleotides at the 3′ end of the template strand and at the 5′ end of the primer stabilizes the interaction. According to the structural predictions and the results of DNase I footprinting using RTs with deletions

Table 3: Misinsertion Fidelity of Wild-Type and Mutant RTs, as Obtained Using DNA/DNA Template−Primers[a]

enzyme	insertion (T:P)[b]	template−primer D2/PG5			template−primer D2-47/PG5-25		
		k_{cat} (min^{-1})	K_m (μM)	misinsertion ratio f_{ins}[c]	k_{cat} (min^{-1})	K_m (μM)	misinsertion ratio f_{ins}[c]
WT RT	A:T	3.07 ± 0.54	0.173 ± 0.027	1	3.26 ± 0.22	0.065 ± 0.008	1
	A:C	0.45 ± 0.03	1173 ± 209	2.2×10^{-5}	0.45 ± 0.11	899.0 ± 65.0	1.0×10^{-5}
	A:G	0.24 ± 0.06	403.5 ± 124.9	3.4×10^{-5}	0.67 ± 0.32	552.4 ± 230.5	2.4×10^{-5}
	A:A	<0.02	nd[d]	$<2 \times 10^{-6}$	<0.02	nd[d]	$<2 \times 10^{-6}$
R557*	A:T	5.31 ± 1.96	0.110 ± 0.018	1	4.63 ± 1.07	0.062 ± 0.009	1
	A:G	0.58 ± 0.20	338.5 ± 99.9	3.6×10^{-5}	0.63 ± 0.22	240.6 ± 79.0	3.5×10^{-5}
S553*	A:T	9.91 ± 3.60	0.169 ± 0.019	1	5.11 ± 1.37	0.074 ± 0.014	1
	A:G	1.15 ± 0.12	691.8 ± 156.5	2.8×10^{-5}	0.54 ± 0.16	471.4 ± 134.2	1.6×10^{-5}
D549*	A:T	9.27 ± 3.86	0.211 ± 0.030	1	5.49 ± 0.52	0.126 ± 0.022	1
	A:G	1.07 ± 0.11	487.9 ± 187.0	5.0×10^{-5}	0.47 ± 0.14	357.9 ± 97.8	3.0×10^{-5}
N545*	A:T	5.30 ± 1.70	0.162 ± 0.022	1	5.53 ± 2.64	0.085 ± 0.011	1
	A:G	0.53 ± 0.10	267.7 ± 55.2	6.0×10^{-5}	0.37 ± 0.14	298.4 ± 81.5	1.9×10^{-5}
G541*	A:T	2.59 ± 0.81	0.184 ± 0.013	1	3.19 ± 0.34	0.183 ± 0.025	1
	A:C	0.33 ± 0.04	692.0 ± 159.0	3.4×10^{-5}	0.44 ± 0.14	908.0 ± 340.0	2.8×10^{-5}
	A:G	0.28 ± 0.04	492.4 ± 144.1	4.0×10^{-5}	0.16 ± 0.02	467.3 ± 124.6	2.0×10^{-5}
	A:A	<0.02	nd[d]	$<2 \times 10^{-6}$	<0.02	nd[d]	$<2 \times 10^{-6}$

[a] After formation of the RT−DNA/DNA complex, D2/PG5 elongation reactions were incubated at 37 °C for 30 s, except for the incorporation of C opposite to A, which was measured after a 3 min incubation. D2-47/PG5-25 elongation reactions were incubated for 20 s for the incorporation of T, 90 s for G, and 3 min for C. Data shown are the mean values ± standard deviation obtained from a nonlinear least-squares fit of the kinetics data to the Michaelis−Menten equation. Each of the experiments was performed independently at least three times. [b] The first base indicates the template nucleotide at position +1, and the second base indicates the nucleotide incorporated in the assay. [c] $f_{ins} = [k_{cat}(\text{incorrect})/K_m(\text{incorrect})]/[k_{cat}(\text{correct})/K_m(\text{correct})]$. [d] Not determined because incorporation of dATP was too low to obtain kinetic values. Misinsertion ratios in this case were estimated by assuming a K_m similar to that observed with dGTP or dCTP.

Table 4: Mispair Extension Fidelity of Wild-Type and Mutant RTs, as Obtained Using DNA/DNA Template−Primers[a]

enzyme	base pair at the 3′ end[b]	template−primer D2/PG5			template−primer D2-47/PG5-25		
		k_{cat} (min^{-1})	K_m (μM)	mispair extension ratio f_{ext}[c]	k_{cat} (min^{-1})	K_m (μM)	mispair extension ratio f_{ext}[c]
WT RT	A:T	3.07 ± 0.54	0.173 ± 0.027	1	3.26 ± 0.22	0.065 ± 0.008	1
	A:C	2.32 ± 0.98	35.1 ± 9.6	3.8×10^{-3}	2.54 ± 0.38	7.9 ± 1.3	6.4×10^{-3}
	A:G	0.23 ± 0.05[d]	0.13 ± 0.04[d]	10.1×10^{-2} [d]	0.031 ± 0.020	>100	$<6.2 \times 10^{-6}$
	A:A	0.40 ± 0.02[d]	0.14 ± 0.03[d]	15.4×10^{-2} [d]	0.020 ± 0.008	>50	$<8.0 \times 10^{-6}$
R557*	A:T	5.31 ± 1.96	0.110 ± 0.018	1	4.63 ± 1.07	0.062 ± 0.009	1
	A:C	5.64 ± 1.32	21.3 ± 4.2	5.5×10^{-3}	4.01 ± 0.49	11.9 ± 3.0	4.5×10^{-3}
S553*	A:T	9.91 ± 3.60	0.169 ± 0.019	1	5.11 ± 1.37	0.074 ± 0.014	1
	A:C	10.83 ± 0.79	22.8 ± 4.3	8.1×10^{-3}	4.93 ± 0.53	15.5 ± 3.1	4.6×10^{-3}
D549*	A:T	9.27 ± 3.86	0.211 ± 0.030	1	5.49 ± 0.52	0.126 ± 0.022	1
	A:C	12.64 ± 0.80	28.0 ± 4.2	10.3×10^{-3}	5.20 ± 0.91	15.0 ± 2.6	7.9×10^{-3}
N545*	A:T	5.30 ± 1.70	0.162 ± 0.022	1	5.53 ± 2.64	0.085 ± 0.011	1
	A:C	3.51 ± 0.27	19.4 ± 4.3	5.5×10^{-3}	4.80 ± 2.24	14.2 ± 1.0	5.2×10^{-3}
G541*	A:T	2.59 ± 0.81	0.184 ± 0.013	1	3.19 ± 0.34	0.183 ± 0.025	1
	A:C	1.79 ± 0.33	14.3 ± 2.7	8.9×10^{-3}	2.46 ± 0.29	22.3 ± 5.6	6.3×10^{-3}
	A:G	nd[e]	nd	nd	0.021± 0.005	>100	$<1.2 \times 10^{-5}$
	A:A	nd	nd	nd	0.019 ± 0.003	>50	$<2.2 \times 10^{-5}$

[a] After formation of the RT−DNA/DNA complex, mispair extension reactions with D2/PG5 were incubated at 37 °C during 30 s for the elongation of A:T and A:C pairs. Extensions of D2-47/PG5-25 were carried out for 20 s for the elongation of A:T and A:C and 7 min for A:G and A:A mispairs. In all cases we measured the incorporation of T opposite to A at position +1. Data shown are the mean values ± standard deviation obtained from a nonlinear least-squares fit of the kinetics data to the Michaelis−Menten equation. Each of the experiments was performed independently at least three times. [b] The first base corresponds to the template and the second base to the primer. [c] $f_{ext} = [k_{cat}(\text{mismatched})/K_m(\text{mismatched})]/[k_{cat}(\text{matched})/K_m(\text{matched})]$. [d] These data were taken from ref 25. [e] Not determined.

of 8 or 16 residues (*21*), the α-helix E′ of the RNase H domain contributes to the wall of the nucleic acid binding cleft. The results presented in this paper indicate that truncations affecting residues of α-helix E′ lead to a moderate decrease in the binding affinity of RT and duplex DNA. This effect is observed with both DNA/DNA template−primers. The loss of interaction sites between RT and template−primer appears to be a plausible explanation for the results obtained with the 47/25mer and truncated RTs. However, the available crystallographic data of a 19/18mer DNA/DNA complexed with HIV-1 RT (*8*, *9*) suggest that the 5′ end of the primer and the 3′ end of the template in the 38/16mer complex used in our experiments would not interact with α-helix E′. It is not known whether the 38/16mer duplex would adopt the same conformation as the 19/18mer in the RT nucleic acid binding cleft. If it does, the decrease of affinity observed with the 38/16mer could be explained assuming a conformational change affecting template−primer binding, which would appear as a consequence of the stepwise deletion of α-helix E′.

The removal of 20 amino acids or fewer of the C-terminal end of p66 did not have a major effect on the specific polymerase activity of HIV-1 RT, in agreement with data reported by other authors (*21*, *22*, *40*). Ghosh et al. (*21*) have shown that the deletion of the last 8 residues affects RNase H activity and impairs strand transfer. Site-directed

Table 5: Misinsertion Fidelity of Wild-Type RT and Mutant G541* Using the RNA/DNA Template Primer D2-47(RNA)/PG5-25[a]

enzyme	insertion (T:P)[b]	k_{cat} (min^{-1})	K_m (μM)	misinsertion ratio f_{ins}[c]
WT RT	A:T	1.11 ± 0.31	0.059 ± 0.030	1
	A:C	0.124 ± 0.026	380.5 ± 174.2	1.7×10^{-5}
	A:G	0.031 ± 0.011	738.5 ± 276.6	2.3×10^{-6}
	A:A	0.019 ± 0.010	544.1 ± 208.6	1.9×10^{-6}
G541*	A:T	0.86 ± 0.30	0.074 ± 0.026	1
	A:C	0.093 ± 0.037	430.3 ± 314.2	1.8×10^{-5}
	A:G	0.028 ± 0.011	701.0 ± 221.6	3.4×10^{-6}
	A:A	0.015 ± 0.005	688.2 ± 163.3	1.9×10^{-6}

[a] After formation of the RT−RNA/DNA complex, elongation reactions were incubated at 37 °C for 20 s for the incorporation of T opposite to A, 60−90 s for C, and 5 min for A and G. Data shown are the mean values ± standard deviation obtained from a nonlinear least-squares fit of the kinetics data to the Michaelis−Menten equation. Each of the experiments was performed independently at least three times. [b] The first base indicates the template nucleotide at position +1, and the second base indicates the nucleotide incorporated in the assay. [c] $f_{ins} = [k_{cat}(\text{incorrect})/K_m(\text{incorrect})]/[k_{cat}(\text{correct})/K_m(\text{correct})]$.

Table 6: Mispair Extension Fidelity of Wild-Type RT and Mutant G541* Using the RNA/DNA Template Primer D2-47(RNA)/PG5-25[a]

enzyme	base pair at the 3′ end[b]	k_{cat} (min^{-1})	K_m (μM)	mispair extension ratio f_{ext}[c]
WT RT	A:T	1.11 ± 0.31	0.059 ± 0.030	1
	A:C	0.77 ± 0.07	4.2 ± 0.6	9.8×10^{-3}
	A:G	0.106 ± 0.039	27.3 ± 12.9	2.0×10^{-4}
	A:A	0.054 ± 0.014	9.1 ± 2.3	3.0×10^{-4}
G541*	A:T	0.86 ± 0.30	0.074 ± 0.026	1
	A:C	0.48 ± 0.03	10.7 ± 2.3	3.9×10^{-3}
	A:G	0.057 ± 0.014	17.3 ± 5.1	2.8×10^{-4}
	A:A	0.030 ± 0.006	10.3 ± 6.7	2.5×10^{-4}

[a] After formation of the RT−RNA/DNA complex, mispair extension reactions were incubated at 37 °C during 20 s, for the elongation of the A:T and A:C pairs, and during 7 min for the extension of A:G and A:A mispairs. In all cases we measured the incorporation of T opposite to A at position +1. Data shown are the mean values ± standard deviation obtained from a nonlinear least-squares fit of the kinetics data to the Michaelis−Menten equation. Each of the experiments was performed independently at least three times. [b] The first base corresponds to the template and the second base to the primer. [c] $f_{ext} = [k_{cat}(\text{mismatched})/K_m(\text{mismatched})]/[k_{cat}(\text{matched})/K_m(\text{matched})]$.

mutagenesis of amino acid residues involved in template−primer binding showed that several residues such as Trp-229, Met-230, Tyr-232, Gly-262, or Trp-266 may have an important role in polymerase activity and/or fidelity of DNA synthesis (*11*−*18*). Our data on the misinsertion and mispair extension fidelity using both DNA/DNA template−primers did not reveal significant differences between all enzymes tested. Misinsertion ratios were on the order of 10^{-5}−10^{-6}, within the range of values reported by other authors (*4, 41*−*43*). Misincorporation efficiencies with both DNA/DNA complexes were higher for C and G opposite to A and almost negligible for the formation of A:A mispairs. The similar f_{ins} values of C and G reveal certain unspecificity in the formation of transition or transversion mispairs. This phenomenon appears not to be related to the size of the template−primer but could be influenced by the conformation of the template strand, since formation of A:G mismatches was less efficient when the template strand was RNA. Mispair extension ratios were around 10^{-3} for A:C mispairs and 10^{-5}−10^{-6} for A:A and A:G mispairs, using the 47/25mer complexes containing DNA or RNA templates. These values are in good agreement with data reported by other authors using template−primers of different sizes (*41, 44, 45*). A:C mispair extension ratios were also similar in assays done with the 38/16mer DNA/DNA complex, although in this case transversion mispair extensions were unusually high (*25*). Nevertheless, in both cases (using 47/25mer or 38/16mer DNA/DNA complexes), the selectivity of transversion mispair extension was mostly influenced by decreasing the k_{cat} for the incorporation of the next nucleotide.

The comparison of fidelity of RNA- and DNA-dependent DNA synthesis of HIV-1 RT remains a controversial issue. Error rate estimates based on genetic assays conflict as to whether RNA-dependent or DNA-dependent polymerization is more precise. Hübner et al. (*46*) conclude that the synthesis with an RNA template is less accurate than with a DNA template, whereas Boyer et al. (*47*) suggest the opposite. In contrast, others have reported a similar fidelity of DNA synthesis with both types of templates (*48, 49*). It is possible that these disparities result from the differences in experimental strategies or in the sequences used in different experiments. Few reports deal with comparisons based on kinetic measurements of nucleotide incorporation using RNA/DNA and DNA/DNA complexes. Thus, pre-steady-state kinetics of polymerization using template−primers of identical size (45/25mers) and sequence revealed a higher fidelity of mismatch formation for RNA-dependent DNA synthesis (*50*). Steady-state kinetic assays carried out with template−primers bearing the same sequence at the insertion site did not reveal major differences in misincorporation and mispair extension fidelity of DNA synthesis, using RNA or DNA templates (*41*−*43*). One of the major limitations of all of these studies lies in the intrinsic endonuclease activity of WT RT. When an RNA/DNA duplex is incubated with the enzyme in the presence of Mg^{2+}, internal cleavage of the template strand occurs, diminishing the significance of the comparison between RNA and DNA templates of identical size. Misinsertion and mispair extension fidelity assays rendered similar results with WT RT and with mutant G541*. However, G541* is devoid of RNase H activity. The comparison of misincorporation and mispair

extension ratios of G541* using D2-47/PG5-25 or D2-47-(RNA)/PG5-25 revealed that fidelity of DNA synthesis was roughly similar using both template−primers, with misinsertion ratios of 10^{-5}−10^{-6} and mispair extension ratios of 10^{-3}−10^{-4}. However, differences were observed in the misinsertion of G instead of T, which occurs 10 times more efficiently with the DNA template, and in the extension of transversion mispairs (e.g., A:A and A:G), which is more efficient with the RNA template. Similar results were obtained with WT RT, suggesting that the endonucleolytic cleavage of the template strand may not produce significant alterations in the positioning of the primer terminal nucleotide and its 3′-OH group at the polymerase active site.

In summary, this study has shown that (i) the size of the double-stranded DNA duplex has a moderate stabilizing effect on the interaction of the template−primer with WT RT and mutants with truncations affecting α-helix E′ of RNase H domain, and (ii) partial or total removal of α-helix E′ weakens the interaction of RT and nucleic acid substrate. Despite the observed differences in template−primer binding, fidelity of DNA synthesis using RNA or DNA templates remains largely unaffected by the deletion of the 20 residues at the C-terminal region of p66, which include α-helix E′. The α-helix E′, together with the C-terminal residues of p51 and viral factors such as the nucleocapsid protein (*21*, *51*), plays a role in strand transfer and retroviral recombination. The question remains whether the truncated mutants described in this paper would have an altered fidelity of strand transfer.

ACKNOWLEDGMENT

I thank E. Arnold and J. Ding for providing the complete coordinates of HIV-1 RT complexed with a 19/18mer double-stranded DNA template−primer, prior to their release by the Brookhaven Protein Data Bank (entry 2HMI). I am also grateful to students and monitors of the Third Master Course on Biotechnology (Universidad Autónoma of Madrid) for technical assistance and discussion at the early stages of this project, to A. Mas for critically reading the manuscript, and to E. Domingo for valuable suggestions and support.

REFERENCES

1. Arts, E. J., and Wainberg, M. A. (1996) *Adv. Virus Res. 46*, 97−163.
2. Hottiger, M., and Hübscher, U. (1996) *Biol. Chem. Hoppe-Seyler 377*, 97−120.
3. Telesnitsky, A., and Goff, S. P. (1997) in *Retroviruses* (Coffin, J. W., Hughes, S. H., and Varmus, H. E., Eds.) pp 121−160, Cold Spring Harbor Laboratory Press, Plainview, NY.
4. Preston, B. D., Poiesz, B. J., and Loeb, L. A. (1988) *Science 242*, 1168−1171.
5. Roberts, J. D., Bebenek, K., and Kunkel, T. A. (1988) *Science 242*, 1171−1173.
6. Ricchetti, M., and Buc, H. (1990) *EMBO J. 9*, 1583−1593.
7. Kohlstaedt, L. A., Wang, J., Friedman, J. M., Rice, P. A., and Steitz, T. A. (1992) *Science 256*, 1783−1790.
8. Jacobo-Molina, A., Ding, J., Nanni, R. G., Clark, A. D., Jr., Lu, X., Tantillo, C., Williams, R. L., Kamer, G., Ferris, A. L., Clark, P., Hizi, A., Hughes, S. H., and Arnold, E. (1993) *Proc. Natl. Acad. Sci. U.S.A. 90*, 6320−6324.
9. Ding, J., Hughes, S. H., and Arnold, E. (1997) *Biopolymers 44*, 125−138.
10. Hermann, T., Meier, T., Götte, M., and Heumann, H. (1994) *Nucleic Acids Res. 22*, 4625−4633.
11. Jacques, P. S., Wöhrl, B. M., Ottmann, M., Darlix, J. L., and Le Grice, S. F. J. (1994) *J. Biol. Chem. 269*, 26472−26478.
12. Ghosh, M., Jacques, P. S., Rodgers, D. W., Ottman, M., Darlix, J.-L., and Le Grice, S. F. J. (1996) *Biochemistry 35*, 8553−8562.
13. Wöhrl, B. M., Krebs, R., Thrall, S. H., Le Grice, S. F. J., Scheidig, A. J., and Goody, R. S. (1997) *J. Biol. Chem. 272*, 17581−17587.
14. Palaniappan, C., Wisniewski, M., Jacques, P. S., Le Grice, S. F. J., Fay, P. J., and Bambara, R. A. (1997) *J. Biol. Chem. 272*, 11157−11164.
15. Beard, W. A., Stahl, S. J., Kim, H.-R., Bebenek, K., Kumar, A., Strub, M.-P., Becerra, S. P., Kunkel, T. A., and Wilson, S. H. (1994) *J. Biol. Chem. 269*, 28091−28097.
16. Beard, W. A., Minnick, D. T., Wade, C. L., Prasad, R., Won, R. L., Kumar, A., Kunkel, T. A., and Wilson, S. H. (1996) *J. Biol. Chem. 271*, 12213−12220.
17. Gao, H.-Q., Boyer, P. L., Arnold, E., and Hughes, S. H. (1998) *J. Mol. Biol. 277*, 559−572.
18. Bebenek, K., Beard, W. A., Casas-Finet, J. R., Kim, H.-R., Darden, T. A., Wilson, S. H., and Kunkel, T. A. (1995) *J. Biol. Chem. 270*, 19516−19523.
19. Wöhrl, B. M., Tantillo, C., Arnold, E., and Le Grice, S. F. J. (1995) *Biochemistry 34*, 5343−5350.
20. Davies, J. F., II, Hostomska, Z., Hostomsky, Z., Jordan, S. R., and Matthews, D. A. (1991) *Science 252*, 88−95.
21. Ghosh, M., Howard, K. J., Cameron, C. E., Benkovic, S. J., Hughes, S. H., and Le Grice, S. F. J. (1995) *J. Biol. Chem. 270*, 7068−7076.
22. Tisdale, M., Schulze, T., Larder, B. A., and Moelling, K. (1991) *J. Gen. Virol. 72*, 59−66.
23. Martín-Hernández, A. M., Domingo, E., and Menéndez-Arias, L. (1996) *EMBO J. 15*, 4434−4442.
24. Quiñones-Mateu, M. E., Soriano, V., Domingo, E., and Menéndez-Arias, L. (1997) *Virology 236*, 364−373.
25. Martín-Hernández, A. M., Gutiérrez-Rivas, M., Domingo, E., and Menéndez-Arias, L. (1997) *Nucleic Acids Res. 25*, 1383−1389.
26. Reardon, J. E. (1992) *Biochemistry 31*, 4473−4479.
27. Patel, P. H., Jacobo-Molina, A., Ding, J., Tantillo, C., Clark, A. D., Jr., Raag, R., Nanni, R. G., Hughes, S. H., and Arnold, E. (1995) *Biochemistry 34*, 5351−5363.
28. Boosalis, M. S., Petruska, J., and Goodman, M. F. (1987) *J. Biol. Chem. 262*, 14689−14696.
29. Ricchetti, M., and Buc, H. (1993) *EMBO J. 12*, 387−396.
30. Wang, J., Smerdon, S. J., Jäger, J., Kohlstaedt, L. A., Rice, P. A., Friedman, J. M., and Steitz, T. A. (1994) *Proc. Natl. Acad. Sci. U.S.A. 91*, 7242−7246.
31. Furfine, E. S., and Reardon, J. E. (1991) *J. Biol. Chem. 266*, 406−412.
32. Gopalakrishnan, V., Peliska, J. A., and Benkovic, S. J. (1992) *Proc. Natl. Acad. Sci. U.S.A. 89*, 10763−10767.
33. Metzger, W., Hermann, T., Schatz, O., Le Grice, S. F. J., and Heumann, H. (1993) *Proc. Natl. Acad. Sci. U.S.A. 90*, 5909−5913.
34. Götte, M., Maier, G., Gross, H. J., and Heumann, H. (1998) *J. Biol. Chem. 273*, 10139−10146.
35. Reardon, J. E., Furfine, E. S., and Cheng N. (1991) *J. Biol. Chem. 266*, 14128−14134.
36. Hsieh, J.-C., Zinnen, S., and Modrich, P. (1993) *J. Biol. Chem. 268*, 24607−24613.
37. DeStefano, J. J., Bambara, R. A., and Fay, P. J. (1993) *Biochemistry 32*, 6908−6915.
38. Kati, W. M., Johnson, K. A., Jerva, L. F., and Anderson, K. S. (1992) *J. Biol. Chem. 267*, 25988−25997.
39. Divita, G., Müller, B., Immendörfer, U., Gautel, M., Rittinger, K., Restle, T., and Goody, R. S. (1993) *Biochemistry 32*, 7966−7971.
40. Hizi, A., McGill, C., and Hughes, S. H. (1988) *Proc. Natl. Acad. Sci. U.S.A. 85*, 1218−1222.
41. Yu, H., and Goodman, M. F. (1992) *J. Biol. Chem. 267*, 10888−10896.

42. Bakhanashvili, M., and Hizi, A. (1992) *Biochemistry 31*, 9393−9398.
43. Bakhanashvili, M., and Hizi, A. (1993) *Biochemistry 32*, 7559−7567.
44. Perrino, F. W., Preston, B. D., Sandell, L. L., and Loeb, L. A. (1989) *Proc. Natl. Acad. Sci. U.S.A. 86*, 8343−8347.
45. Bakhanashvili, M., and Hizi, A. (1992) *FEBS Lett. 304*, 289−293.
46. Hübner, A., Kruhoffer, M., Grosse, F., and Krauss, G. (1992) *J. Mol. Biol. 223*, 595−600.
47. Boyer, J. C., Bebenek, K., and Kunkel, T. A. (1992) *Proc. Natl. Acad. Sci. U.S.A. 89*, 6919−6923.
48. Ji, J., and Loeb, L. A. (1992) *Biochemistry 31*, 954−958.
49. Ji, J., and Loeb, L. A. (1994) *Virology 199*, 323−330.
50. Kerr, S. G., and Anderson, K. S. (1997) *Biochemistry 36*, 14056−14063.
51. Cameron, C. E., Ghosh, M., Le Grice, S. F. J., and Benkovic, S. J. (1997) *Proc. Natl. Acad. Sci. U.S.A. 94*, 6700−6705.

BI981830G